13th World Conference on Earthquake Engineering
Vancouver, B.C., Canada
August 1-6, 2004
Paper No. 1981

EXPERIMENTAL STUDY ON SEISMIC RETROFITTING OF MASONRY WALLS USING GFRP

Dagen WENG[1], Xilin LU[2], Changdong ZHOU[3], Tetsuo KUBO[4] and Kangning LI[5]

SUMMARY

The experimental study, performed on brick masonry walls strengthened or repaired with Glass Fiber Reinforced Polymer (GFRP) sheets or steel-mesh reinforced cement mortar, and aimed to investigate the efficiency of an alternative seismic resistance reinforcement technique is introduced in this paper. A series of 13 unreinforced masonry walls strengthened with GFRP sheets were tested under cyclic shear and constant axial load. Different reinforcement configurations were evaluated. Experimental results pointed out that GFRP and steel-mesh reinforcement did significantly modify the shear collapse mechanisms (diagonal splitting), ductility behavior and energy dissipation capacity of the unreinforced masonry. Performances of the different reinforcement configurations are compared in terms of strength, ductility and failure mechanism.

INTRODUCTION

As is known, in unreinforced masonry walls, failure in brittle, shear rupture occurs either as a diagonal splitting or as step-pattern sliding along the mortar joints, depending on the characteristics of the constituent materials (mortar and bricks). Therefore, in order to predict the masonry shear capacity, it is necessary to first identify the most anticipated failure mechanism, based on the knowledge of the involved materials.

Presently, many methods are successfully used as reinforcement in masonry retrofitting, such as steel-mesh reinforced cement mortar layer, RC tie columns and beams, etc. These traditional methods generally need much time and construction cost, so engineers are trying to find some new methods and materials to solve these problems.

Nowadays, FRP sheets represent a new opportunity in restoring field, with considerable development in unreinforced masonry strengthening. FRP have received significant attentions for use in civil

[1] Professor, State Key Laboratory for Disaster Reduction in Civil Engineering, Tongji University, P. R. China. Email: wdg@mail.tongji.edu.cn
[2] Professor, Tongji University, P. R. China. Email: lxlst@mail.tongji.edu.cn
[3] Post Doctor, Tongji University, P. R. China. Email: zhouchangdong@163.com
[4] Professor, Earthquake Disaster Mitigation Research Center, Japan. Email:kubo@archi.ace.nitech.ac.jp
[5] Engineer, Canny Structural Analysis (CSA), Canada. Email: kangning@shaw.ca

infrastructure due to their unique properties, such as the high strength-to-weight ratio and stiffness-to-weight ratio, corrosion and fatigue resistance, and tailor ability. The strengthening method is to glue FRP sheets to the surface of masonry substrate by epoxy resin. Its construction is simple and express, so it can be used to retrofit damaged masonry structures in earthquake or other historical buildings to avoid added loss.

A certain number of FRP masonry strengthening applications have already been performed, involving either CFRP or GFRP sheets. GFRP is suitable material to strengthening masonry structures in China for its high mechanical property and low price, but few analytical or experimental research works have been done to investigate the effectiveness and reliability of that new technology.

In the present experimental work, which was performed on different reinforcement configurations, 13 different masonry walls strengthened or repaired with steel-mesh reinforced cement mortar layer, low-strength and high-strength GFRP were tested under cyclic lateral load and constant axial load. The purpose of the tests is to analyze the effectiveness of shear resistance in-plane mechanisms of collapse.

TEST DESIGN OF WALL SPECIMENS

Material properties

As mentioned, masonry mechanical properties depend on the characteristics of the constituent elements (bricks and mortar), as well as on the workmanship and the interface interaction within the assemblage. Properties of GFRP sheets used in test were listed in Table 1. The characteristic compressive strength of brick is 10MPa. The cube strength of mortar was listed in Table 2.

Table 1 Physical and mechanical characteristics of the GFRP sheets

Type of fiber	Thickness (mm)	Width (cm)	Tensile strength (MPa)	Ultimate strain (%)	Tensile modulus of elasticity (MPa)
CW130-1000 (low-strength, bidirection)	0.13	90	98.4	0.94	1.22×10^4
EGFW430 (high-strength, unidirection)	0.169	60	2.04×10^3	2.4	9.31×10^4

Specimen description

A series of 13 masonry walls having nominal dimensions of 240×1500×3000 mm （thickness×height ×width）were built in five groups in different time due to the limitation of casting site. Design cube strength of mortar and observed strength of mortar were listed in Table 2. The values in brackets are observed strength.

The specimens were made of solid clay bricks (240mm×115mm×53mm) and have 10-mm-thick mortar joints. Each specimen has 23 layers of brick, and is referred from the base to the top as layer 1 to layer 23. In the streamline procedure the same patch of mortar is used to lay the brick of the same layers for all. To ensure the reliability and comparability of the test results among the specimens, the same worker is employed to lay the bricks simultaneously for all specimens of the same group using the same mortar.

To study the influence of the eccentricity of the strengthening, the GFRP sheets were applied on both sides or only at one side of the walls. All the GFRP sheets were bonded along with axial direction. The strengthening pattern is shown in Table 2.

In Table 2, different superior figures represented different reinforcement program. From 1 to 7, each figure represents masonry walls repaired with GFRP, strengthened with GFRP, strengthened with steel-

mesh reinforced cement layer, strengthened with high-strength GFRP at one side with 1-layer, strengthened with high-strength GFRP at one side with 2-layer, strengthened with high-strength GFRP at two-side with 1-layer, and strengthened with high-strength GFRP at two-side with 2-layer, respectively.

Table 2 Description of the specimens

Design cube strength of mortar (MPa)	Vertical stress in walls			
	σ_0=0.2	σ_0=0.6	σ_0=0.8	σ_0=1.0
2.5	X102 (2.19) RX102[1](2.19)	R106GF[2](1.46),R106N[3](1.46) HR1106GF[4](1.5), HR1206GF[5](1.5) HR2106GF[6](1.5), HR2206GF[7](1.5)	X108 (2.35)	—
5	X202 (5.09)	X206 (5.09)	X208 (5.09)	XX210 (3.88) RXX210[1](3.88) X210 (5.09)
10	—	—	—	Y210 (9.75)
15	—	—	X308 (18.2) RX308[1](18.2)	—

All the specimens can be divided into five types, listed in the following:

(1) Masonry walls as built: Only a thin layer of mortar was laid on double-side of masonry walls. For better crack-watching, a thin white lime mortar coating was painted on the surface of specimens.

(2) Masonry walls repaired with low-strength GFRP: They were repaired with low-strength GFRP (CW130-1000). Two-layer GFRP sheets were glued to the two-side surface of damaged specimens in the former test.

(3) Masonry walls strengthened with low-strength GFRP: These specimens were bonding 2-layer low-strength GFRP sheets to the surface of "as built" walls by epoxy resin.

(4) Masonry walls strengthened with steel-mesh reinforced cement layer: Steel wire diameter is 4mm, mortar thickness is from 35mm to 40mm. Steel wire ends were implanted into top beam and footing beam, infixing length is no less than 50mm. Arrangement plan of steel wires and strains bonded on the wires was listed in Fig. 1.

(5) Masonry strengthened with high-strength GFRP (EGFW430) and low-strength GFRP (CW130-1000).

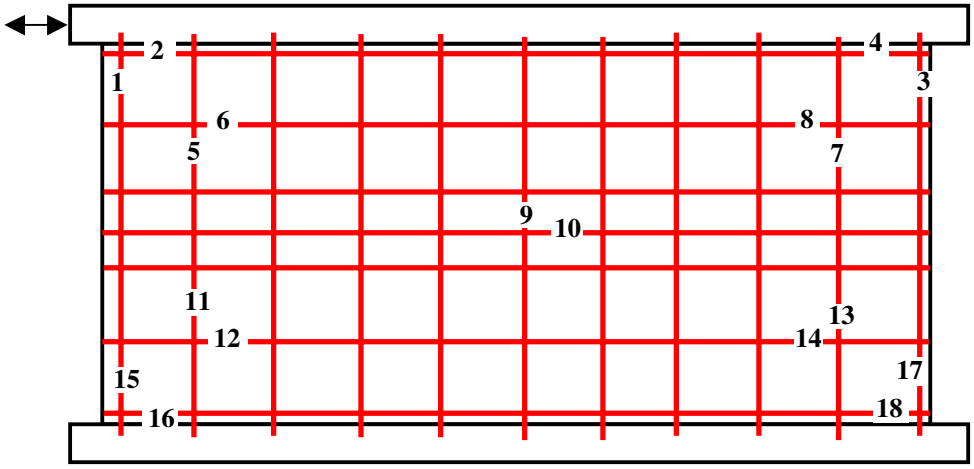

Fig. 1 Steel wires arrangement plan of R106N specimen

Table 1 shown that the strength of the former is 20-time of the latter, tensile elasticity modulus of the former is 7.62 times of the latter.

Test setup

The test setup is shown in Fig. 2. As shown in Figure 2, the specimen of masonry wall is laid on an I-shaped RC footing beam, which was fixed on the lab floor. The masonry wall is topped by a RC beam. The top RC beam has a slight stud at the two ends to hold the masonry wall. Lateral cyclic load is applied to the specimens by Instron Schenck Testing System (IST), and constant axial load is provided by oil jacks mounted on the top beam of specimens.The vertical load through the jacks is first applied up to the designed value at the beginning of the test, and then is kept as constant load during the test. The lateral loading path is designed as following.

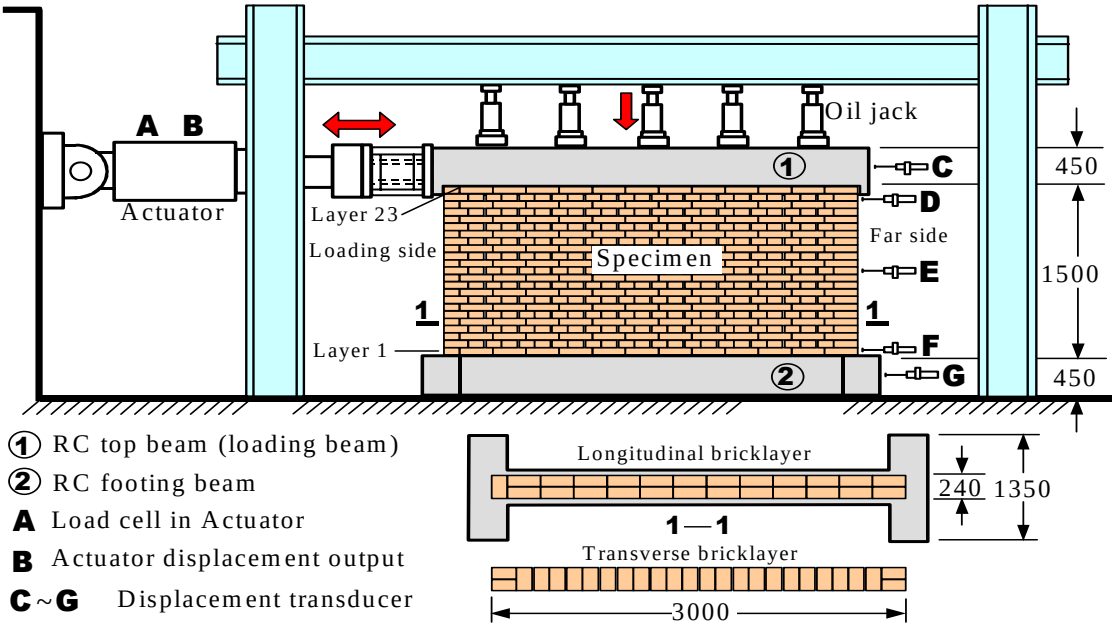

Fig. 2 Illustration of the loading test system and specimen outline

(1) Before reaching the estimated specimen maximum resistance P_u, the loading is controlled by a load increment $\Delta P = P_u/10$ for each loading step.

(2) After reaching the estimated resistance P_u, the stroke of the actuator is controlled at a displacement increment $\Delta D = D_u/2$ for each loading step. Where D_u is the lateral displacement at the estimated resistance P_u.

(3) For the specimen subjected to static cyclic loading, load-time curve of sin-function is used. The time for each loading cycle is 50 seconds and is kept constant throughout the test.

However, during the loading test, the displacement of the specimen is always monitored even in the load steps using load increment control, and the loading control is shifted from load increment ΔP control to displacement increment ΔD control when the lateral load has reached 70 % of the estimated maximum resistance P_u, thus to avoid the failure of loading control due to too large load (in the case of over estimated resistance P_u). As the result, there are different loading steps for each specimen. The loading test is continued until severe cracks occurred in the masonry wall, and is terminated when the specimen is about to collapse.

EXPERIMENTAL RESULTS AND ANALYSIS

Failure modes of specimens

Masonry walls as built

The crack forms may be divided into three types: X cracking shape, appeared in X102, X208, Y210, XX210 (see Fig. 3); ladder-shape cracking, corresponding to X206, X308 (see Fig. 4); horizontal crack between brick, appeared in X202 and X108.

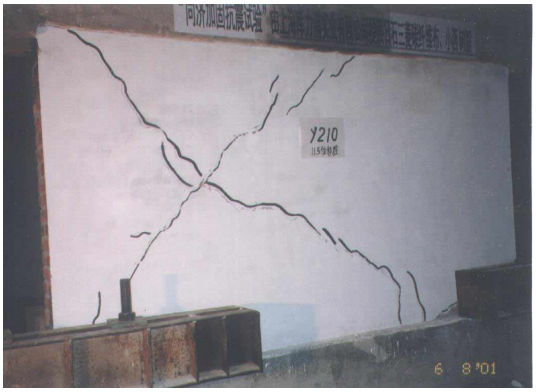

Fig. 3 X-shape cracking of masonry

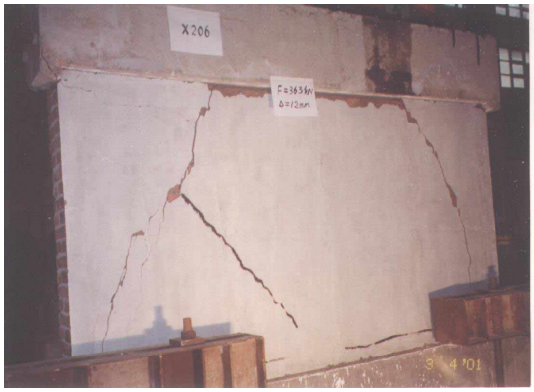

Fig. 4 Ladder-shape cracking of masonry

When reaching maximum load, specimen X202 has had out-plane slipping. The test had to be terminated when there was 22 mm out-plane movement. This is attributed to the relative smaller normal stress for the specimen and the original cracks between the masonry wall and the footing beam due to accident collision when setting up the specimen.

For specimen X108, oblique cracks occurred in the wall base on both sides. At the place of one-third of wall height, the oblique cracks developed along horizontal direction. Finally the horizontal cracks of both sides met together. These cracks were ladder-shaped. This also is a damaged specimen. Otherwise the cracking shape should be X. The maximum residual crack width reached 8~38mm.

Damaged masonry walls repaired with low-strength GFRP

Specimens of RX102, RX308 and RXX210 were repaired with low-strength GFRP after specimens of X102, X308 and XX210 damaged. Failure modes of these specimens are the developing of original crack. After GFRP ruptured, the bearing capacity of specimens declined sharply.

Intact masonry walls strengthened with low-strength GFRP

Specimen of R106GF was strengthened with low-strength GFRP. Its cracking shape is X. Residual crack width reached 19mm (see Fig. 5 and 6).

Masonry walls strengthened with steel-mesh reinforced cement layer

Specimen of R106N was strengthened with steel-mesh reinforced cement layer. Its cracking shape is also X. Residual crack width is little. Footing wall brick severely crushed, cement mortar layer spilled and steel wires were exposed (see Fig. 7 and 8).

Masonry strengthened with high-strength GFRP sheets

Specimens strengthened with high-strength GFRP include four masonry walls, HR1106GF（one-side with 1-layer）, HR1206GF（one-side with 2-layer）, HR2106GF（two-side with 1-layer）and HR2206GF (two-side with 2-layer). The cracking shapes of the first three specimens are all X, but the last

is ladder. Although brick wall were severely damaged, GFRP sheets did not rupture. GFRP tore along with fiber direction at last. Brick of walls popped out and mortar crushed in test.

Fig. 5 Cracking of masonry strengthened with low-strength GFRP

Fig. 6 Enlarged view of cracking

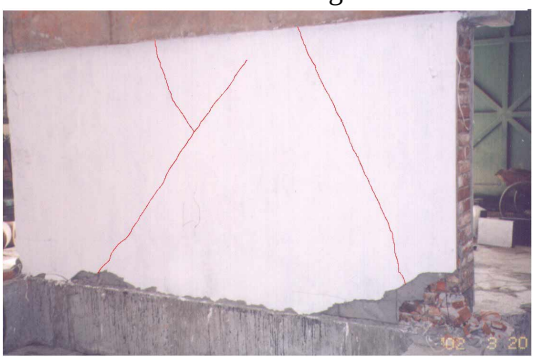

Fig.7 Cracking of masonry strengthened with steel-mesh

Fig.8 Crushing of footing wall brick in specimen strengthened with steel-mesh

One-side strengthening

Splitting failure with a clear X crack pattern was also obtained in all one-side reinforced masonry walls, ultimate load of specimen HR1206GF was 1.189-time of HR1106GF (see Fig. 9 ~ 10, HR1206GF had the same crack pattern). The failure mode of specimens was brick splitting. In the test process, rupture and debonding of GFRP sheets was not been found.

Fig. 9 Masonry failure mode in HR1106GF

Fig. 10 GFRP failure mode in HR1106GF

Two-side strengthening

In the specimen HR2106GF, failure mode is still the splitting of masonry substrate (see Fig. 11), and few GFRP sheets were rupture and debonding in the test process. But for specimen HR2206GF, the failure reason is the sudden loss of collaboration between reinforcement and substrate due to debonding of the superficial part of masonry (see Fig. 12). The unreinforced masonry typical sudden failure was noticeably improved by the GFRP strengthening, where crack wide spreading provided sufficient signals of incipient crisis well before collapse.

Fig. 11 Failure mode of HR2106GF

Fig. 12 Failure mode HR2206GF

Failure of interface

In all cases the rupture was due to detachment of the brick superficial skin. Tore out GFRP sheets from the masonry, a piece of mortar and brick was bonded on the surface of GFRP sheets (see Fig. 13). Even a few bricks were drawn out from masonry.

Crushing of footing wall brick

In the test process, we could see that footing wall brick was always been crushed at first (see Fig.14). Then the crack width of masonry began to develop rapidly. Finally, brick split and specimen was totally damaged.

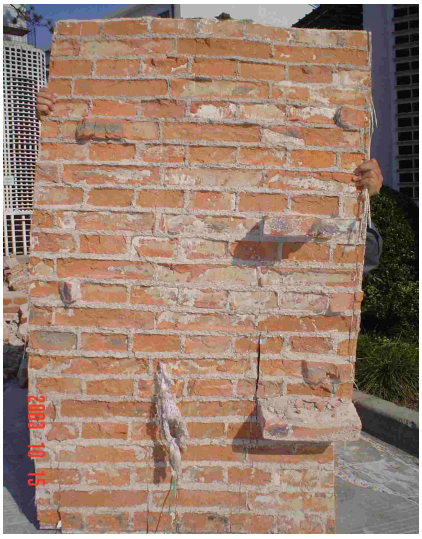

Fig. 13 Failure mode of interface

Fig. 14 Crushing of footing wall brick

Test analysis

According to formula 7.2.8-1 in Code for Seismic Design of Buildings [2], we can calculate the design seismic resistant strength of unreinforced masonry step-pattern sliding along the mortar joints.

$$V \le f_{vE} A / \gamma_{RE} \quad (1)$$

V — design shear force of masonry walls;

f_{vE} —design seismic resistant strength of unreinforced masonry along with trapezoid cross section, can be calculated by formula (2);

A — sectional area of walls;

γ_{RE} — adjustment coefficient of bearing capacity.

$$f_{vE} = \zeta_N f_v \quad (2)$$

f_v —design shear strength of masonry in the case of no earthquake-resistance see reference [1];

ζ_N — shear strength normal stress influence coefficient of masonry, given in Table 7.2.7 in reference [2].

Substituted mortar strength and normal stress into formula (1), we can get the value of V , listed in Table 3.

Table 3 Comparison between test ultimate strength of masonry and calculation result

Specimen	σ_0 (MPa)	f_v (MPa)	ζ_N	$V(kN)$	$P_{u1}(kN)$	$\lambda_0 = P_{u1}/V$		
X102	0.2+0.07	0.08	1.322	76	247	3.25	Mean 3.24	Mean 3.06 （excluding X202、X108）
X202*	0.2+0.07	0.11	1.203	95	341	3.59		
X206	0.6+0.07	0.11	1.609	127	363	2.86		
X108*	0.8+0.07	0.08	2.015	116	482	4.16		
X208	0.8+0.07	0.11	1.776	141	423	3.00		
X308	0.8+0.07	0.17	1.512	185	402	2.17		
XX210	1.0+0.07	0.10	1.928	153	573	3.75		
X210	1.0+0.07	0.11	1.944	154	543	3.53		
Y210	1.0+0.07	0.17	1.629	199	571	2.87		

In Table 3, 0.07MPa in σ_0 is normal stress generated by weight of top beam and 0.5 weight of wall; * denoted that specimenX202 and X108 were damaged before test, the test loads were abnormal.

Ultimate bearing capacity P_{u2} of repaired masonry walls and P_{u2} / P_{u1} are shown in Table 4. We can see that the strength of masonry walls repaired with GFRP almost reach their original strength.

Table 4 Comparison of P_{u1} and P_{u2}

Repaired specimen （original specimen ）	σ_0 (MPa)	$P_{u1}(kN)$	$P_{u2}(kN)$	$\lambda_1 = P_{u2} / P_{u1}$	
RX102（X102）	0.2+0.07	247	238	0.96	Mean: 1.01
RXX210（XX210）	1.0+0.07	573	485	0.85	
RX308（X308）	0.8+0.07	402	491	1.22	

The test loads of reinforcement masonry were listed in Table 5. According to reference [1] and [2], with mortar strength 1.46MPa and normal compressive stress of walls, following results can be got, as

$f_v = 0.07, \zeta_N = 1.65$， $V = 83.2kN$ and $P_{u1} = 255kN$. The shear strength of strengthened masonry increased. The effectiveness is related to strengthening method. We can draw the following conclusions.

(1) The effectiveness of steel-mesh at two-side of masonry walls is the better than strengthened with high-strength two-side GFRP. The effectiveness of one-side with 2-layer high-strength GFRP is almost equal to two-side with 2-layer low-strength GFRP.

(2) Comparing the ultimate load of H1206GF and H2106GF, the effectiveness of two-side is better than one-side.

Table 5 Cracking load and ultimate load P_{u2}

Specimen	$\sigma_0(MPa)$	$P_{u1}(kN)$	Cracking load（kN）	$P_{u2}(kN)$	$\lambda_1 = P_{u2} / P_{u1}$
R106GF	0.6+0.07	255	250	370	1.45
R106N	0.6+0.07	255	430	550	2.16
HR1106GF	0.6+0.07	255	170	300	1.18
HR1206GF	0.6+0.07	255	220	380	1.49
HR2106GF	0.6+0.07	255	300	430	1.69
HR2206GF	0.6+0.07	255	300	480	1.88

Total thickness of GFRP is $t_G = 4 \times 0.13$. Its ratio related to equivalence thickness of masonry is:

$$E_G t_G / E_W t_W = 1.46 \times 10^{-2} \quad (3)$$

Where, $E_W = 1807N/mm^2$， $E_G = 12210N/mm^2$. At first, masonry shared most tensile force. If tensile stress in some position is more than its ultimate tensile stress, masonry cracked, then GFRP have to share tensile stress of cracked masonry. With growing of load, GFRP ruptured and tore out from wall surface, and crack developed. Tensile capacity of GFRP approximated to $P_G = f_{Fib} t_G L = 154kN$. It is less than cracking capacity of undamaged walls. Equivalence thickness of one layer high-strength GFRP related to brick is:

$$E_G^H t_G^H / E_W t_W = 3.6 \times 10^{-2} \quad (4)$$

One layer ultimate tensile capacity of high-strength GFRP can be calculated as $P_G = f_{Fib}^H t_G^H L = 1034kN$. It is much more than the ultimate load of undamaged masonry. So GFRP did not rupture in test process. As shown in Table 5~7, with the help of GFRP, in specimen HR1106GF, HR1206GF and HR2106GF, crack can be developed sufficiently, and the bearing capacity and energy dissipating capacity can also be enhanced. Stiffness and integrity of specimen HR2206GF were also be improved by two-side with 2-layer high-strength GFRP. Considering the cost, specimen of two-side with 1-layer is the best.

Specimen R106N was strengthened with steel-mesh reinforced cement mortar layer. The thickness of mortar layer related to brick is:

$$E_C t_C / E_W t_W = 4.1 \quad (5)$$

Where, $E_C = 25500N/mm^2, t_C = 70mm$. This strengthening method can add sectional area of walls and increase cracking load. In elastic phase, steel-mess and mortar layer may bear load commonly. The bearing capacity of R106N is 200KN larger than R106GF. It is the effectiveness of steel-mesh reinforced cement mortar layer.

Table 6 Test results of displacement

Specimen	Cracking displacement (mm)	Displacement according to failure load(mm)			Growth rate (%)
		Forward	Backward	Even	
HR1106GF	10	5.9	-8.9	7.4	100.0

HR1206GF	12	9. 5	-8.8	9.1	123.2
HR2106GF	16	12.2	-13.4	12.8	172.3
HR2206GF	16	12.2	-12.6	12.4	166.4

Table 7 Energy dissipating capacity of specimen

Specimen	Dissipative capacity（KN-mm）	Growth rate (%)
HR1106GF	14300	100.0
HR1206GF	25031	175.0
HR2106GF	40740	284.9
HR2206GF	40971	286.5

Hysteretic curves

Hysteretic curves were given in Fig.15~17 based on the relative lateral displacement (equal to top beam displacement subtracting footing beam displacement) and lateral load. Fig.15~17 shown that stiffness and bearing capacity all degraded. Through integral transformation, energy dissipating capacity of each specimen was got. The results were listed in Table 7.

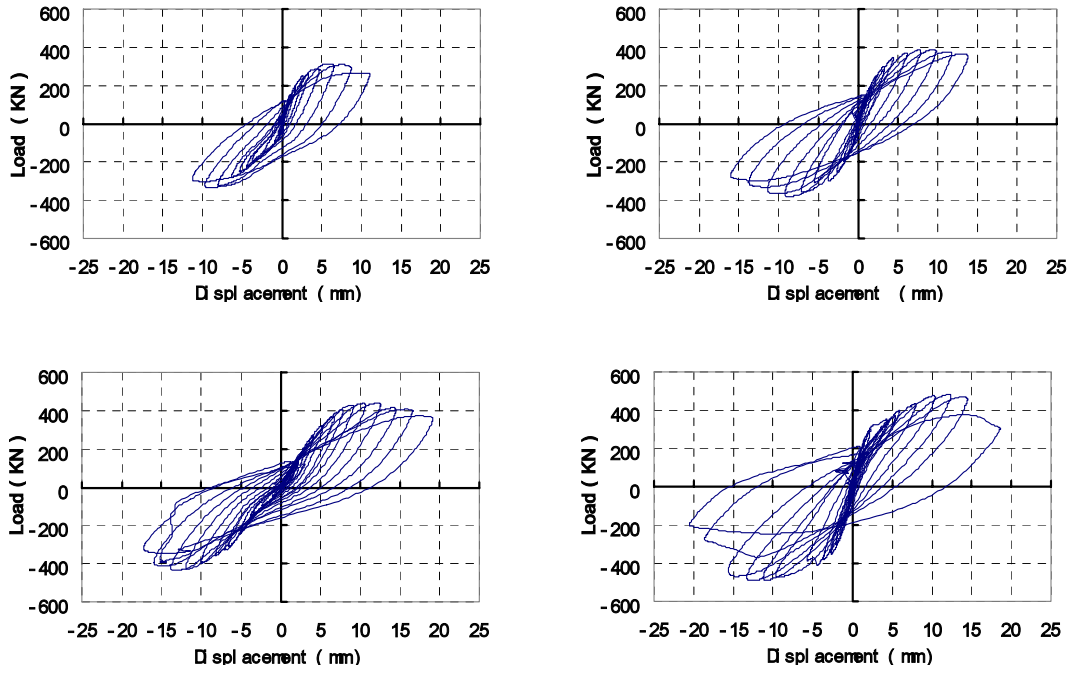

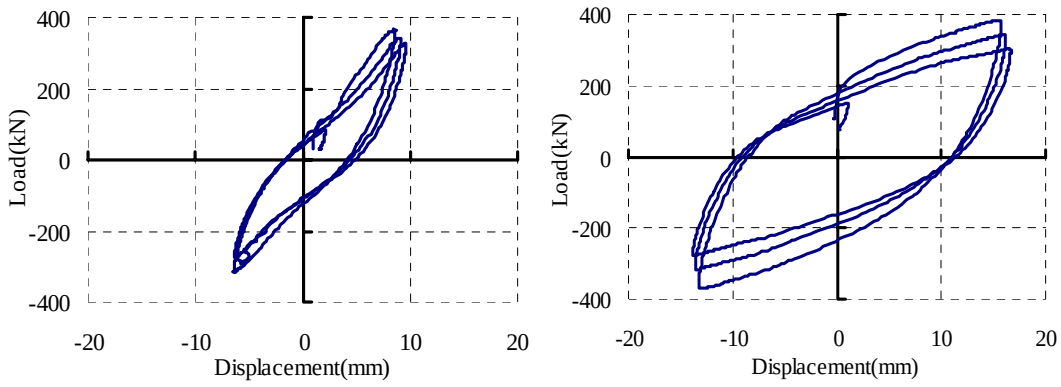

Test results indicate that the energy dissipating capacity of masonry can be highly improved by bonding GFRP sheets. It also shown that GFRP sheets can significantly enhanced seismic resistance and ductility behavior of specimens.

Both one-side and two-side configurations can modify the behavior of masonry, and growth rate of energy dissipating capacity is from 175% to 286.5%. The test results shown that the latter is more effective than the former. The energy dissipating capacity of two-side with 1-layer specimen is almost equal to that of two-side with 2-layer specimen, but the ductility of the former is less than the latter (see Fig.15 (c) and (d)).

Skeleton curves

According to ultimate load and corresponding displacement of each loading cycle, skeleton curves of specimens were drawn and shown in Fig. 18~22, respectively.

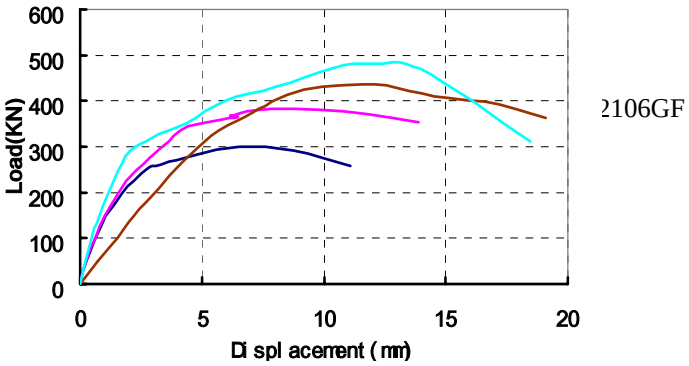

From Fig.18, a significant growth of stiffness can be seen for the masonry walls strengthened by means of bonding GFRP sheets. But the stiffness of HR2106GF, strengthened with two layers GFRP sheets, is much less than HR1106GF and HR1206GF (corresponding to specimen strengthened with 1-layer and 2-layer GFRP sheets). The reason maybe is experimental error or inhomogeneity of materials.

Fig. 19 and 20 shown that the higher the normal stress of specimen, the larger the ultimate shear strength is the wall maintains in the case of same strength mortar. As compressive stress equivalence, mortar strength is less important to ultimate lateral load than compressive stress.

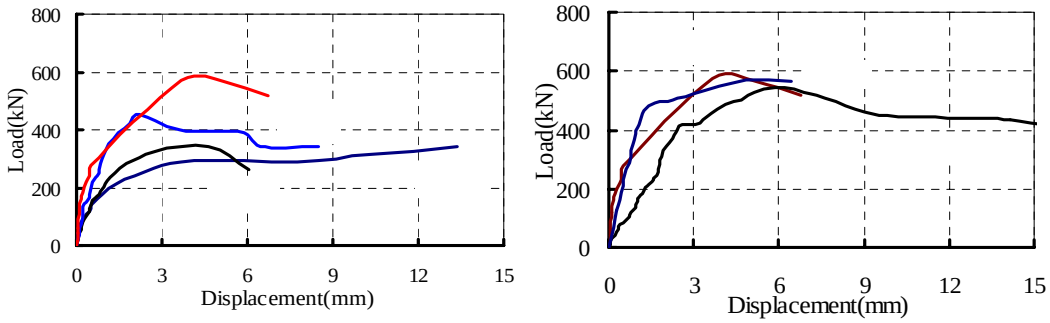

Fig. 19 Skeleton curves of different compressive stress

Fig.21 shown that ultimate shear strength of specimens repaired walls almost reached the strength of original masonry walls.

Fig.22 clearly shown that original stiffness of R106N is much more than that of R106GF, and displacement according to failure load of R106N is much less than that of R106GF.

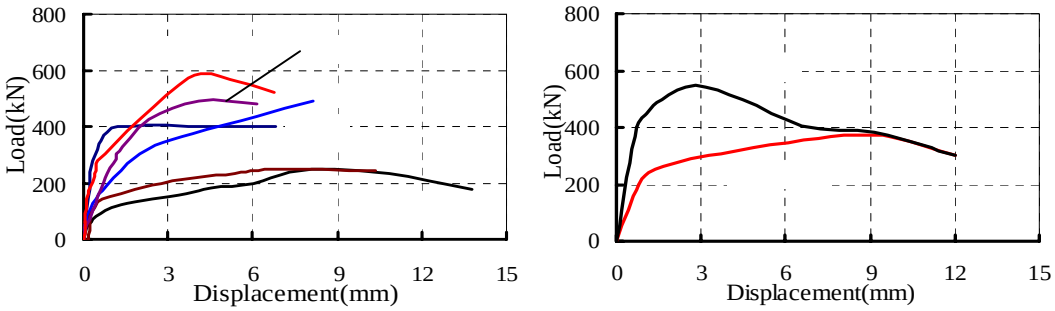

Fig. 21 Skeleton curves of repaired and original walls

CONCLUSIONS

（1） Ultimate shear capacity of walls is directly proportional to vertical compressive stress;

（2） Integrity of masonry walls can be effectively improved by boding low-strength GFRP. Mortar can be reinforced by GFRP. Because GFRP is a type of brittle material, energy dissipating capacity of specimens still depends on the friction in masonry walls;

（3） High-strength GFRP can not only enhance integrity of masonry walls, but also can improve shear strength and energy dissipating capacity of specimens. The effectiveness of two-side GFRP is better than that of one-side. Since high-strength GFRP did not rupture in all the test phase, GFRP guaranteed that vertical bearing capacity did not suddenly lost after brick damaged. So the ductility behavior of specimens was improved by high-strength GFRP.

（4） Integrity, stiffness and lateral bearing capacity of masonry can be improved by strengthening with steel-mesh reinforced cement mortar. Anchorage length of vertical steel wire should be assured to maintain its effectiveness;

（5） Footing walls brick damaged in all tests, although crack width was very fine (see Fig. 7) after strengthened. In this case, the shear capacity of walls depends on local compressive strength of masonry.

ACKNOWLEDGMENTS

The experimental research was supported by the EDM EqTAP Project and the research fund from Shanghai Government. The loading test was carried out in the State Key Laboratory for Disaster Reduction in Civil Engineering at Tongji University. The authors would like to express their sincere thanks to the lab staff for their efforts in completing the test.

REFERENCES

1. China National Standard: Code for masonry structures (GB 50003-2001), China Building Industry Press, 2001. (in Chinese)
2. China National Standard: Code for seismic design of buildings (GB 50011-2001), China Building Industry Press, 2001. (in Chinese)
3. WENG Da-gen, LU Xi-lin, REN Xiao-song, Tetsuo KUBO, LI Kang-ning. “Experimental Study on Seismic Resistant Capacity of Repaired and Strengthened Masonry Walls.”World Earthquake Engineering, March 2003, 19 (1): 1-8.(in Chinese)